

PAPER • OPEN ACCESS

## Reduced texture approach for crystal plasticity finite element method toward macroscopic engineering applications

To cite this article: D Noh and J W Yoon 2020 *IOP Conf. Ser.: Mater. Sci. Eng.* **967** 012071

View the [article online](#) for updates and enhancements.

### You may also like

- [Void growth in high strength aluminium alloy single crystals: a CPFEM based study](#)  
Umair Asim, M Amir Siddiq and Murat Demiral
- [Modelling the plastic anisotropy of aluminum alloy 3103 sheets by polycrystal plasticity](#)  
K Zhang, B Holmedal, O S Hopperstad et al.
- [Grain refinement in the equal channel angular pressing process: simulations using the crystal plasticity finite element method](#)  
Karol Frydrych and Katarzyna Kowalczyk-Gajewska



**ECS**  
The  
Electrochemical  
Society  
Advancing solid state &  
electrochemical science & technology

**DISCOVER**  
how sustainability  
intersects with  
electrochemistry & solid  
state science research

# Reduced texture approach for crystal plasticity finite element method toward macroscopic engineering applications

D Noh<sup>1</sup> and J W Yoon<sup>1,2\*</sup>

<sup>1</sup> Department of Mechanical Engineering, Korea Advanced Institute of Science and Technology, 291 Daehak-ro, Yuseong-gu, Daejeon 34141, Republic of Korea

<sup>2</sup> School of Engineering, Deakin University, Geelong Waurn Ponds, VIC 3220, Australia

E-mail: [j.yoon@kaist.ac.kr](mailto:j.yoon@kaist.ac.kr), [j.yoon@deakin.edu.au](mailto:j.yoon@deakin.edu.au)

**Abstract.** In Crystal Plasticity Finite Element Method (CPFEM), normally over thousands Euler angles are used. It leads to high computational cost. To efficiently solve this problem, a reduced texture approach was implemented through User MATerial Interface (UMAT). Specific material parameters including the texture information were calibrated to characterize anisotropic behavior. For the calibration, it is used the stress-strain curves and r-values along the rolling, diagonal, and transverse directions. In this study, AA 2090-T3 was modelled with the reduced texture approach by characterizing 12 parameters. Single element simulation result from the reduced texture approach shows a good agreement with the experimental data. In addition, a deep drawing simulation for AA 2090-T3 was performed. The simulation results from the reduced texture approach were compared with those from the advanced constitutive models such as Yld2000-2d and Yld2004-18p in terms of accuracy and time efficiency. It shows a great potential that the reduced texture approach based on the crystal plasticity theory could be applied to macroscopic engineering problems as an alternative solution for continuum level advanced constitutive models.

## 1. Introduction

In large scale engineering applications, many grains are employed for CPFEM leading to texture mapping problems. The major issue is how to map the intensive information of crystallographic orientations to integration points. In the view of computational cost, it is inefficient to use the huge amount of grains in CPFEM. Therefore, an effective way of mapping of crystallographic orientations to the integration points is recommended for the large scale CPFEM.

Many research has been devoted to achieve reasonable computational cost with the reduction of crystallographic orientations. Among them, a reduced texture methodology was proposed by Rousselier et al. [1, 2]. In the work, a strongly anisotropic and an initially isotropic material were firstly attempted with the self-consistent model. Moreover, the ductile fracture of sheet metals and the multi-axial deformation with the strength-differential effect were predicted with the reduced texture methodology [3, 4]. However, many parameters were required to implement the reduced texture methodology.

In this study, a reduced texture approach was implemented with simple crystal plasticity constitutive model instead of the self-consistent model. Therefore, the number of parameters was reduced. To describe anisotropic behavior, total 12 parameters were calibrated using a single element simulation. In addition, a circular cup drawing simulation was performed and simulation results were evaluated in terms of accuracy and time efficiency.



Content from this work may be used under the terms of the [Creative Commons Attribution 3.0 licence](https://creativecommons.org/licenses/by/3.0/). Any further distribution of this work must maintain attribution to the author(s) and the title of the work, journal citation and DOI.

## 2. Crystal plasticity model

In this study, the crystal plasticity model described by Yoon et al. [5] was used. Total deformation gradient ( $\mathbf{F}$ ) is decomposed into the elastic ( $\mathbf{F}^e$ ) and plastic ( $\mathbf{F}^p$ ) parts as shown in Equation (1).

$$\mathbf{F} = \mathbf{F}^e \cdot \mathbf{F}^p \quad (1)$$

The velocity gradient ( $\mathbf{L}$ ) is also decomposed into the elastic ( $\mathbf{L}^e$ ) and plastic ( $\mathbf{L}^p$ ) parts, i.e.,

$$\mathbf{L} = \dot{\mathbf{F}} \cdot \mathbf{F}^{-1} = \dot{\mathbf{F}}^e \cdot (\mathbf{F}^e)^{-1} + \mathbf{F}^e \cdot \dot{\mathbf{F}}^p \cdot (\mathbf{F}^p)^{-1} \cdot (\mathbf{F}^e)^{-1} = \mathbf{L}^e + \mathbf{L}^p \quad (2)$$

Because the plastic velocity gradient is the result of the shear strain contributions over all the slip systems, it can be expressed as:

$$\mathbf{L}^p = \sum_{\alpha=1}^{NSYS} \dot{\gamma}^{(\alpha)} \mathbf{s}^{(\alpha)} \otimes \mathbf{m}^{(\alpha)} \quad (3)$$

where  $NSYS$  is the number of the slip systems,  $\dot{\gamma}^{(\alpha)}$  is the slip rate, and  $\mathbf{s}^{(\alpha)}$  and  $\mathbf{m}^{(\alpha)}$  are the vectors along the slip direction and normal direction of the slip plane. When the constitutive relations are formulated, the objectivity should be satisfied. The Jaumann rate is generally used as the objective stress rate and the Jaumann rate of the Kirchhoff stress was well derived by Kim and Yoon [6]. After calculating the Jaumann rate of the Kirchhoff stress, the stress state at the grain level is updated, i.e.,

$$\boldsymbol{\tau}_{n+1} = \mathbf{R} \cdot \boldsymbol{\tau}_n \cdot \mathbf{R}^T + \Delta t \tilde{\boldsymbol{\tau}} \quad (4)$$

where  $\tilde{\boldsymbol{\tau}}$  is the Jaumann rate of the Kirchhoff stress and  $\mathbf{R}$  is the rotation tensor which is obtained from the polar decomposition.

In this study, rate dependent hardening behavior was used to compute the slip rate and the phenomenological models were employed as follows:

$$\dot{\gamma}^{(\alpha)} = \dot{\gamma}_0 \cdot \left[ \frac{|\boldsymbol{\tau}_{rss}^{(\alpha)}|}{g^{(\alpha)}} \right]^{\frac{1}{m}} \cdot \text{sign}(\boldsymbol{\tau}_{rss}^{(\alpha)}) \quad (5)$$

where  $\dot{\gamma}_0$  is the reference slip rate,  $\boldsymbol{\tau}_{rss}^{(\alpha)}$  is the resolved shear stress,  $m$  is the rate sensitivity, and  $g^{(\alpha)}$  is the slip resistance. Also, the slip resistances are evolved as follows:

$$\dot{g}^{(\alpha)} = \sum_{\beta=1}^{NSYS} h^{\alpha\beta} |\dot{\gamma}^{\beta}| \quad (6)$$

$$h^{\alpha\beta} = qh + (1-q)h\delta_{\alpha\beta} \quad (7)$$

$$h = h_{\infty} + (h_0 - h_{\infty}) \text{sech}^2 \left[ \left( \frac{h_0 - h_{\infty}}{g_{\infty} - g_0} \right) \cdot \gamma \right] \quad (8)$$

where  $h_0, h_{\infty}$  are the initial and saturated hardening rates,  $g_0, g_{\infty}$  are the initial and saturated value of the slip resistances,  $q$  describes the latent hardening, and  $\gamma$  is the summation of the slips over all the slip systems. In addition, the stress state at integration point level is volume averaged:

$$\boldsymbol{\sigma} = \sum_{g=1}^N f_g \boldsymbol{\sigma}_g \quad (9)$$

where  $N$  indicates the number of grains in each integration point,  $g$  means each grain, and  $f_g$  is the volume fraction of  $g$ .

### 3. Reduced texture approach

#### 3.1. Experimental data

In this study, AA 2090-T3 was modelled. The stress ratios ( $s_\theta = \sigma_\theta / \sigma_0$ ) where  $\sigma_\theta$  indicates the stress anisotropy in  $\theta$  degree from the rolling direction and r-values were measured from the tensile tests conducted along the rolling, diagonal, and transverse directions. The results are shown in Table 1 [2]. However, the complete experimental data does not exist. The experimental data were built by using the yield stress ratios, r-values, and the stress-strain hardening curve along the rolling direction. Therefore, the stress-strain curves in  $\theta$  degree from the rolling direction were defined as:

$$\bar{\sigma}_\theta = 646 \left( 0.025 + \bar{\varepsilon}^p \right)^{0.227} \cdot s_\theta \quad (10)$$

In addition, the transverse strain curves are shown in Figure 1(b) assuming that r-values are independent of the strain value. All of the data were built up to  $\bar{\varepsilon}^p = 0.28$  to implement large strain results into deep drawing simulations.

**Table 1.** Experimental results of AA 2090-T3.

	Rolling	Diagonal	Transverse
Stress ratio	1.0000	0.8148	0.9115
r-value	0.20	1.57	0.70

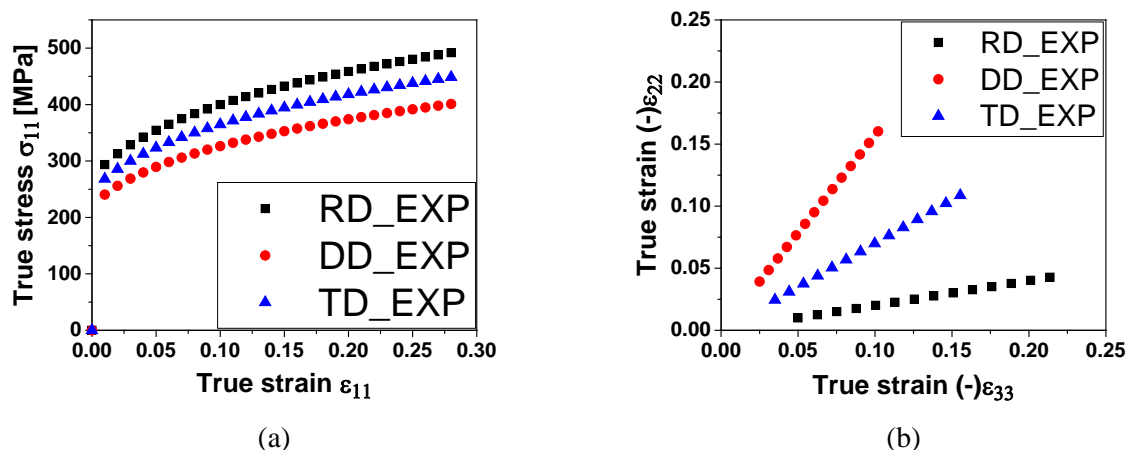


**Figure 1.** Experimental data used for parameter calibration: (a) stress-strain curves; (b) transverse strain curves.

#### 3.2. Calibration

Parameters were calibrated with Abaqus2016/Standard and Isight2016. The experimental data used for parameter calibration were as follows:

- Stress-strain curves along the rolling, diagonal, and transverse directions
- Transverse strain curves along the rolling, diagonal, and transverse directions

Total six curves were used for material characterization. For material constants, the rate sensitivity was set to  $m = 0.04$  because the aluminium alloy is almost rate independent at the room temperature. For the reference slip rate,  $\dot{\gamma}_0 = 0.001$  [1/s] was employed. Elasticity tensor constants for aluminium alloy were set to  $C_{1111} = 108000$ ,  $C_{1122} = 62000$ ,  $C_{1212} = 28300$  [MPa]. In the framework of the reduced texture approach, there are some parameters related to crystallographic orientations. As shown in the result of Rousselier et al. [1], two texture representatives were employed. For orthotropic symmetry, each texture representative consists of four grains which are expressed as  $(\varphi_1 \ \phi \ \varphi_2)$ ,  $(-\varphi_1 \ \phi \ -\varphi_2)$ ,  $(\varphi_1 \ -\phi \ \varphi_2)$ , and  $(-\varphi_1 \ -\phi \ -\varphi_2)$ . Therefore, total eight grains were included in each integration point. In conclusion, the parameters to be calibrated were as follows:

- Slip resistance ( $h_0, h_\infty, g_0, g_\infty$ , four parameters)
- Grain information ( $\{\varphi_1(1), \phi(1), \varphi_2(1)\}, \{\varphi_1(2), \phi(2), \varphi_2(2)\}, f(1)$ , seven parameters)
- Latent hardening ( $q$ , one parameter)

Total twelve parameters were calibrated for the material characterization. In addition,  $q$  was bounded between 1 and 1.4 [7]. Although it is hard to find the exact latent hardening parameter with only tensile test, it was used as a fitting scheme. Then, Single element tensile simulation was conducted for the parameters' calibration.

The calibrated parameters are shown in Table 2. Figure 2 shows the stress-strain and transverse strain curves from the experimental data and simulation results. The reduced texture approach (CP) shows a good agreement with the experimental data.

**Table 2.** Results of the calibrated parameters.

$g_0$ [MPa]	$g_\infty$ [MPa]	$h_0$ [MPa]	$h_\infty$ [MPa]	$q$	$f(1)$
99.69	130.21	199.32	37.23	1.0470	0.0882
$\varphi_1(1)$ [°]	$\phi(1)$ [°]	$\varphi_2(1)$ [°]	$\varphi_1(2)$ [°]	$\phi(2)$ [°]	$\varphi_2(2)$ [°]
62.66	13.59	51.02	51.08	32.07	4.58

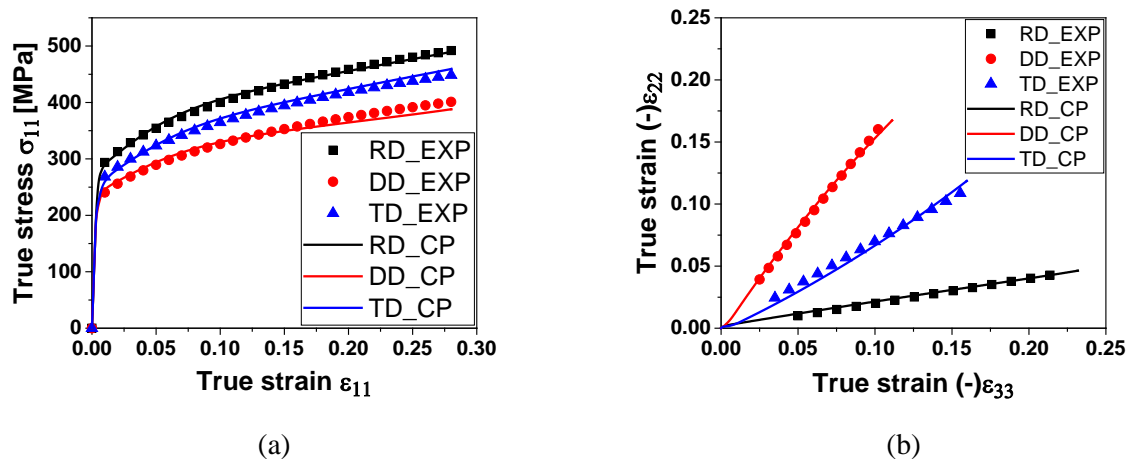


**Figure 2.** Experimental data and simulation results: (a) stress-strain curves; (b) transverse strain curves.

#### 4. Deep drawing simulation

A circular cup drawing simulation was conducted to evaluate the applicability of the reduced texture approach for the large scale engineering problems. The schematic view of the circular cup drawing simulation is illustrated in Figure 3. The dimensions and process variables are specified in Table 3 [8].

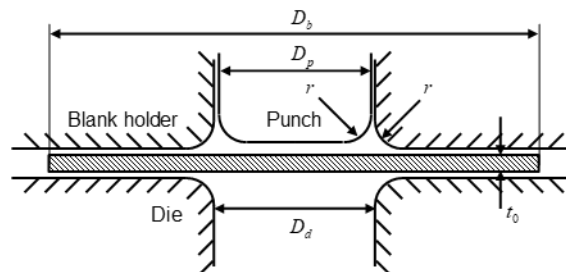


**Figure 3.** Schematic view of the cup drawing simulation.

**Table 3.** Dimensions and process variables for the cup drawing simulation.

Dimension [mm]	
Punch diameter ( $D_p$ )	97.46
Die opening diameter ( $D_d$ )	101.48
Blank diameter ( $D_b$ )	158.76
Fillet radius ( $r$ )	12.70
Initial blank thickness ( $t_0$ )	1.60
Process variables	
Coulomb coefficient of friction	0.1
Blank holding force [kN]	22.2

Because the material was assumed to be orthotropic symmetry, only a quarter section of the blank was analyzed. Total 2400 and 100 elements were employed for C3D8R and C3D6, respectively.

Two comparisons are following; First, the earing profile from the reduced texture approach was compared with that from the Yld2000-2d [9] because both of them used the stress ratios and r-values along the rolling, diagonal, and transverse directions. Second, the computational time from the reduced texture approach was compared with that from the Yld2004-18p since they are based on 3D solid element. The results are shown in Figure 4 and Table 4, respectively. Although the experimental r-value in 75 degree was not used in the reduced texture approach, the current model can predict six earing including a small ear along 15 degree which comes from the r-value in 75 degree from the rolling direction. In addition, the predicted earing profile shows a good agreement with the experimental data. Moreover, the computational time from the current model was less than twice that from the Yld2004-18p.

#### 5. Conclusion

In this study, the reduced texture approach was employed to apply the crystal plasticity theory to large scale engineering problems with reduced computational cost. Specific parameters including texture representatives were calibrated and anisotropic behavior of AA2090-T3 was well described. It is concluded that the reduced texture approach could be a good alternative way to advanced continuum constitutive models such as Yld2000-2d or Yld2004-18p in terms of time efficiency and accuracy.

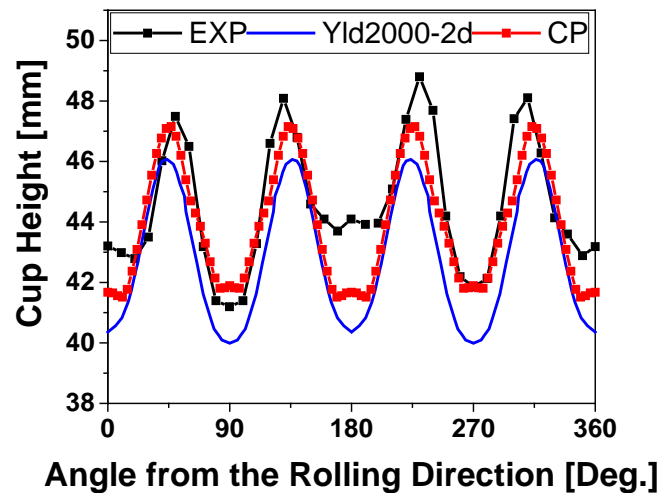


**Figure 4.** The experimental and predicted cup height.

**Table 4.** Normalized simulation time (wallclock time) between the models.

	Yld2004-18p	Reduced texture approach
Normalized simulation time	1.000	1.817

## References

- [1] Rousselier G, Barlat F and Yoon J W 2009 A novel approach for anisotropic hardening modeling. Part I: Theory and its application to finite element analysis of deep drawing *International Journal of Plasticity* **25** 2383-409
- [2] Rousselier G, Barlat F and Yoon J W 2010 A novel approach for anisotropic hardening modeling. Part II: Anisotropic hardening in proportional and non-proportional loadings, application to initially isotropic material *International Journal of Plasticity* **26** 1029-49
- [3] Rousselier G and Luo M 2014 A fully coupled void damage and Mohr–Coulomb based ductile fracture model in the framework of a Reduced Texture Methodology *International Journal of Plasticity* **55** 1-24
- [4] Luo M and Rousselier G 2014 Modeling of large strain multi-axial deformation of anisotropic metal sheets with strength-differential effect using a Reduced Texture Methodology *International Journal of Plasticity* **53** 66-89
- [5] Yoon J W, Barlat F, Gracio J J and Rauch E 2005 Anisotropic strain hardening behavior in simple shear for cube textured aluminum alloy sheets *International Journal of Plasticity* **21** 2426-47
- [6] Kim J-B and Yoon J W 2015 Necking behavior of AA 6022-T4 based on the crystal plasticity and damage models *International Journal of Plasticity* **73** 3-23
- [7] Asaro R J 1983 Crystal plasticity *Journal of applied mechanics* **50** 921-34
- [8] Yoon J W, Barlat F, Dick R and Karabin M 2006 Prediction of six or eight ears in a drawn cup based on a new anisotropic yield function *International Journal of Plasticity* **22** 174-93
- [9] Choi H and Yoon J W 2019 Stress integration-based on finite difference method and its application for anisotropic plasticity and distortional hardening under associated and non-associated flow rules *Computer Methods in Applied Mechanics and Engineering* **345** 123-60